Advanced Physical Research
Vol.8, No.1, 2026, pp.94-101
https://doi.org/10.62476/apr.8194

DEPENDENCE OF ELECTRON RAMAN SPECTRUM OF SEMIMAGNETIC SEMICONDUCTOR $Hg_{1-x}Mn_xTe$ ON CONCENTRATION OF MAGNETIC IONS

Tariyel Ismayilov[1], **Sabina Zeynalova**[1,2*], **S.V. Mahmudova**[3], **E.S. Jafarli**[4]

[1]Baku State University, Baku, Azerbaijan
[2]Institute of Physics of the Ministry of Science and Education of the Republic of Azerbaijan, Baku, Azerbaijan
[3]Nakhchivan State University, Nakhchivan, Azerbaijan
[4]Mingachevir State University, Mingachevir, Azerbaijan

Abstract. The Raman scattering on electronic excitations in $Hg_{1-x}Mn_xTe$ semimagnetic semiconductors (SMS) with inverted band structure is considered in the strong classical magnetic field. The differential cross section (DCS) of the interband Raman scattering is calculated. Since, in the general case, it has a cumbersome form, we present the expression of the DCS only for ZZ geometry. It is shown that DCS depends on the exchange parameters and concentration of magnetic ions. It is found that the resonant peak in the zero magnetic field is split on four lines. This allows us to determine the values of the exchange parameters $N\alpha$ and $N\beta$ consequently, the ratio of these parameters from the values of the resonance frequencies. With the help of obtained formula it is possible to carry out comparative analysis of the magnetic ion concentrations, i.e., the positions of the resonance emission lines can be used to compare different samples and sort them by increasing ion concentrations. Even if one of the parameters are unknown, it is sufficient to record the resonance lines at two values of the magnetic field in order to determine the magnetic ion concentration.

Keywords: Semimagnetic semiconductors, inverted band structure, electron Raman scattering.
Corresponding author: S.I. Zeynalova, Institute of Physics of the Ministry of Science and Education of the Republic of Azerbaijan, Baku, Azerbaijan, Tel.: +994 55 4901234, e-mail: *sebine-zeynalova@mail.ru*
Received: 27 October 2025; Revised: 11 December 2025; Accepted: 25 December 2025; Published: 18 February 2026.

1 Introduction

Diluted magnetic semiconductors (DMS), also known as semimagnetic semiconductors, are a class of materials in which a fraction of the cations in a conventional semiconductor lattice are replaced by magnetic ions, typically transition metals such as manganese (Mn^{2+}) (Soares et al., 2023; Yi Peng et al., 2025). These materials are of significant interest due to their unique ability to couple magnetic and electronic properties within a single crystal structure, making them ideal candidates for studying spin-dependent phenomena and for potential applications in spintronic devices.

Among the most extensively studied DMS materials is Raman scattering on electronic excitations in $Hg_{1-x}Mn_xTe$, a II–VI narrow-gap semiconductor in which divalent manganese ions substitute for mercury in the HgTe host lattice (Harrache & Bouarissa, 2019). The incorporation of Mn introduces localized magnetic moments that interact with conduction electrons and holes via sp–d exchange interactions, significantly modifying the material's electronic and

optical properties. These interactions give rise to phenomena such as giant Zeeman splitting, spin-dependent scattering, and magneto-optical effects, which become increasingly pronounced as the Mn concentration increases.

Electron Raman scattering (ERS) serves as a powerful, non-destructive spectroscopic technique for probing low-energy electronic excitations in semiconductors (Fernández-Lozada et al., 2021; Betancourt-Riera et al., 2023; Aleshkin et al., 2024; Zeynalova & Ismayilov, 2024; Betancourt-Riera et al., 2025). In DMS materials like $Hg_{1-x}Mn_xTe$, ERS provides detailed insight into the interaction between charge carriers and magnetic ions, allowing for the observation of spin-flip processes, energy level shifts, and the effects of magnetic disorder. Variations in the Mn concentration (x) directly influence the ERS spectrum, affecting both the position and intensity of Raman peaks, as well as the appearance of spin-flip Raman scattering (SFRS) features.

This study focuses on investigating the dependence of the electron Raman spectrum of Raman scattering on electronic excitations in $Hg_{1-x}Mn_xTe$ on the concentration of magnetic ions. By systematically analyzing how spectral features evolve with increasing Mn content, we aim to deepen the understanding of exchange interactions and spin-related effects in semimagnetic semiconductors. Such insights are not only relevant for fundamental physics but also crucial for the development of next-generation optoelectronic and spintronic devices. Semimagnetic semiconductors are solid magnetic solutions of semiconductors that contain magnetic ions in low concentrations. Such solid solutions and low-dimensional systems based on them attract attention both from the point of view of fundamental physics and their prospects and great potential for possible applications (Dietl, 2021).

In semimagnetic semiconductors (SMS) Raman scattering on electronic excitations in $Hg_{1-x}Mn_xTe$, $Hg_{1-x}Mn_xSe$, $Cd_{1-x}Mn_xTe$, the carrier spectrum is strongly modified due to the exchange interaction of their spins with the spins of magnetic impurities (Autieri et al., 2020; Cibert & Scalbert, 2017; Miura, 2008). Parameters of electronic states in such semiconductors are easily tuned by changing the concentration of magnetic impurities, temperature, or applied magnetic field. Powerful methods for studying such states are the measurement of resonance absorption of light in an external magnetic field and, especially, electric dipole resonances, as well as Raman scattering (Furdyna & Dobrowolska, 2003).The analysis of the interaction Hamiltonian has shown that the effect of the exchange interaction can be included in already existing models of the energy structures of semiconductors (Mircea Trif et al., 2007; Bastard et al., 1977). It can be assumed that the exchange interaction between the spins of free carriers and localized d-electrons at the node is described (in the molecular approximation) by a Hamiltonian of the Heisenberg type (Bastard et al., 1977):

$$H_{\text{int}} = \sum_{R_i} J(\vec{r} - \vec{R}_i)\, \vec{S}_i \cdot \vec{s}_i. \tag{1}$$

$J(\vec{r} - \vec{R}_i)$- represents the exchange integral centered at the node, $\vec{R}_i$, $\vec{S}_i$ is the spin of the manganese ion, and $\vec{s}_i$ is the carrier's spin. This possibility takes place because the exchange interaction depends only on the electron spin and it can be taken into account by introducing the effective g*-factor, which at low temperatures strongly depends on temperature and can reach enormous values (Autieri et al., 2020; Cibert & Scalbert, 2017; Miura, 2008).

The huge and adjustable values of the g*-factor directly indicate that these materials can be used to fabricate a tunable laser, particularly a spin-flip laser based on Raman scattering (Autieri et al., 2020; Cibert & Scalbert, 2017). Moreover, the study of frequency shifts provides direct information on the value of the g*-factor, as well as on the value of the magnetic ion concentration and the magnitude of the exchange interaction. In the present paper, Raman scattering on electron excitations in semimagnetic semiconductors (SMS) $Hg_{1-x}Mn_xTe$ with inverse band structure in the presence of a classically strong magnetic field is considered.

The calculation of the differential effective section (DCS) of interband Raman scattering

(Fluegel et al., 2015; Burstein et al., 1971) for ZZ geometries is carried out. It is shown that the DCS depends on the exchange parameters and the concentration of magnetic ions. It is found that the peak corresponding to the resonance frequency at H=0 splits into four lines with the inclusion of a magnetic field.

2 Energy spectrum and wave functions of electrons and holes in a classically strong magnetic field

The Hamiltonian taking into account the exchange interaction is written as follows form (Bastard et al., 1977):

$$\hat{H} = \frac{\vec{P}^2}{2m_0} + V(\vec{r}) + \frac{\hbar}{4m_0^2c^2}(\vec{\sigma} \times \nabla V)\vec{p} + \mu_0 \vec{H}\vec{\sigma} + \sum_{R_i} J(\vec{r} - \vec{R}_i) \cdot \vec{S}_i, \tag{2}$$

where $\vec{P} = \vec{p} + \frac{e}{c}\vec{A}$, $\vec{A}$ is the vector-potential of the magnetic field, $\vec{p}$ is the momentum of the free electron, e is the absolute value of the free electron charge, c is the light velocity, m_0 is the mass of a free electron, $\mu_0 = \frac{e\vec{H}}{2m_0c}$ is the Bohr magneton, $\vec{H}$ is the external magnetic field, σ is the Pauli spin operator, with eigenvalues $\vec{\sigma} = \pm 1$, $V(\vec{r})$ is the periodic lattice potential, $\vec{\nabla} = \vec{i}\frac{\partial}{\partial x} + \vec{j}\frac{\partial}{\partial y} + \vec{k}\frac{\partial}{\partial z}$ is the Hamilton operator.

The spin-orbit interaction and the Pauli term are written in the standard form. In the presence of a magnetic field the Hamiltonian (2) is not periodic and one cannot look for its eigen states in the form of the Bloch functions. We shall present here a somewhat simplified derivation of the appropriate equations, trying to find for the eigen value problem (Zawadzki, 1979)

$$\hat{H}\psi(\vec{r}) = \varepsilon\psi(\vec{r}) \tag{3}$$

a solution in the form

$$\psi(\vec{r}) = \sum_l f_l(\vec{r})u_l(\vec{r}), \tag{4}$$

where the summation is over the energy bands, $u_l(\vec{r})$ are the periodic parts of Bloch functions taken at the band's extremum (called the Luttinger-Kohn amplitudes), satisfying the eigen value problem for the Hamiltonian at the same point (k = 0 in our case):

$$u_1 = iS\downarrow\rangle; \quad \varepsilon_{10} = -\varepsilon_g, \qquad u_2 = iS\uparrow\rangle; \quad \varepsilon_{20} = -\varepsilon_g, \tag{5}$$

$$u_3 = \frac{1}{\sqrt{2}}|(X - iY)\downarrow\rangle; \quad \varepsilon_{30} = 0, \quad u_4 = \sqrt{\frac{2}{3}}|Z\downarrow\rangle + \frac{1}{\sqrt{6}}|(X - iY)\uparrow\rangle; \quad \varepsilon_{40} = 0,$$
$$u_5 = \sqrt{\frac{2}{3}}|Z\uparrow\rangle - \frac{1}{\sqrt{6}}|(X + iY)\downarrow\rangle; \quad \varepsilon_{50} = 0, \quad u_6 = \frac{1}{\sqrt{2}}|(X + iY)\uparrow\rangle; \qquad \varepsilon_{60} = 0,$$
$$u_7 = \frac{1}{\sqrt{3}}|Z\downarrow\rangle - \frac{1}{\sqrt{3}}|(X - iY)\uparrow\rangle; \quad \varepsilon_{70} = -\Delta, \quad u_8 = \frac{1}{\sqrt{3}}|Z\uparrow\rangle + \frac{1}{\sqrt{3}}|(X + iY)\downarrow\rangle; \varepsilon_{80} = -\Delta,$$

$$H_0 = \left[\frac{\vec{P}^2}{2m_0} + V(\vec{r}) + \frac{\hbar}{4m_0^2c^2}(\vec{\sigma} \times \nabla V)\vec{P}\right] u_l(\vec{r}) = \varepsilon_l u_l(\vec{r}); \tag{6}$$

ε_l denotes the band edge energies at the center of the Brillouin zone and have the periodicity of the lattice $u_l(\vec{r} + \vec{a}) = u_l(\vec{r})$ and they are orthonormal in the band index that is $\frac{1}{\Omega}\langle u_l|u_{l'}\rangle = \delta_{ll'}$, where the integration is carried over the volume of the unit cell Ω. On the other hand the envelope functions $f_l(\vec{r})$ are slowly varying in coordinate space, extending over many unit cells.

In the two-band Kane model (Teppe, 2016) with taking into account the exchange interaction, we obtain the following equations system:

$$(-E_g - A - \varepsilon) f_1 + 0 \cdot f_2 + xP_- f_3 + \sqrt{\frac{2}{3}} xP_z f_4 - \sqrt{\frac{1}{3}} xP_+ f_5 + 0 \cdot f_6 = 0, \tag{7}$$

$$0 \cdot f_1 + (-E_g + A - \varepsilon) f_2 + 0 \cdot f_3 + \sqrt{\frac{1}{3}} xP_- f_4 + \sqrt{\frac{2}{3}} xP_z f_5 + xP_+ f_6 = 0,$$

$$xP_+ f_1 + 0 \cdot f_2 + (-\varepsilon - B) f_3 + 0 \cdot f_4 + 0 \cdot f_5 + 0 \cdot f_6 = 0,$$

$$\sqrt{\frac{2}{3}} xP_z f_1 + \sqrt{\frac{1}{3}} xP_+ f_2 + 0 \cdot f_3 + \left(-\varepsilon - \frac{B}{3}\right) f_4 + 0 \cdot f_5 + 0 \cdot f_6 = 0,$$

$$-\sqrt{\frac{1}{3}} xP_- f_1 + \sqrt{\frac{2}{3}} xP_z f_2 + 0 \cdot f_3 + 0 \cdot f_4 + \left(-\varepsilon + \frac{B}{3}\right) f_5 + 0 \cdot f_6 = 0,$$

$$0 \cdot f_1 + xP_- f_2 + 0 \cdot f_3 + 0 \cdot f_4 + 0 \cdot f_5 + (-\varepsilon + B) f_6 = 0.$$

Here $P_\pm = \frac{1}{\sqrt{2}}(P_x + iP_y)$, $A = -\frac{\alpha}{2} N_S \langle S_z \rangle$, $B = \frac{\beta}{2} N_S \langle S_z \rangle$, $\langle S_z \rangle = B_{5/2}(g_{Mn} \cdot \mu_0 H / k_0 T)$, where $B_J(x)$ is the Brillouin function corresponding to the total spin J;

$$B_J(x) = [(2J+1)/J \cdot cth(2J+1)/2J]x - (2J)^{-1} cth(x/2J).$$

Solving equations system (7) we find the wave functions for arbitrary $\vec{k}$ and energies spectra the following expressions:

$$\Psi_{ch\downarrow}(\vec{r}) = c_\uparrow \left(u_3 + \sqrt{\frac{2}{3}} \frac{\varepsilon_\downarrow + B}{\varepsilon_\downarrow + B/3} \frac{k_z}{k_+} u_4 + \frac{\varepsilon_\downarrow + B}{\varepsilon_\downarrow + B/3} \frac{k_-}{k_+} u_5 \right) e^{i\vec{k}\vec{r}}, \tag{8}$$

$$\varepsilon_\downarrow = \frac{\hbar^2 k^2}{2m_c} + \frac{B}{3}, c_\downarrow = \left(1 + \frac{4}{3} \frac{\varepsilon_\downarrow + B}{\varepsilon_\downarrow + B/3} \frac{k_z^2}{k_\perp^2} u_4 + \frac{1}{3} \frac{\varepsilon_\downarrow + B}{\varepsilon_\downarrow + B/3} \right), \tag{9}$$

$$\Psi_{ch\uparrow}(\vec{r}) = c_\uparrow \left(u_6 + \frac{1}{\sqrt{3}} \frac{\varepsilon_\uparrow - B}{\varepsilon_\uparrow + B/3} \frac{k_+}{k_-} u_4 - \sqrt{\frac{2}{3}} \frac{\varepsilon_\uparrow - B}{\varepsilon_\uparrow + B/3} \frac{k_z}{k_-} u_5 \right) e^{i\vec{k}\vec{r}}, \tag{10}$$

$$\varepsilon_\uparrow = \frac{\hbar^2 k^2}{2m_c} + \frac{B}{3}, \quad c_\uparrow = \left[1 + \frac{1}{3} \frac{\varepsilon_\uparrow - B}{\varepsilon_\uparrow + B/3} + \frac{4}{3} \frac{\varepsilon_\uparrow - B}{\varepsilon_\uparrow + B/3} \frac{k_z^2}{k_\perp^2} \right]^{-1/2}, \tag{11}$$

$$\Psi_{l\vec{k}\downarrow}(\vec{r}) = u_1 e^{i\vec{k}\vec{r}}, \varepsilon_{l\downarrow} = -\frac{\hbar^2 k^2}{2m_l} - \varepsilon_g + A, \tag{12}$$

$$\Psi_{l\vec{k}\downarrow}(\vec{r}) = u_2 e^{i\vec{k}\vec{r}}, \varepsilon_{l\uparrow} = -\frac{\hbar^2 k^2}{2m_l} - \varepsilon_g - A, \tag{13}$$

$$\Psi_{hk\downarrow}(\vec{r}) = \left(\frac{1}{\sqrt{2}} \frac{k_+}{k} u_3 + \sqrt{\frac{3}{2}} \frac{k_-}{k} u_5 - \frac{k_z}{k} \frac{k_-}{k_+} u_6 \right) e^{i\vec{k}\vec{r}}, \tag{14}$$

$$\varepsilon_\downarrow = -\frac{\hbar^2 k^2}{2m_h} - B, \quad \varepsilon_\downarrow = -\frac{\hbar^2 k^2}{2m_h} + B, \quad k_\pm = k_x \pm ik_y/\sqrt{2}. \tag{15}$$

In (5) to (15), c, l and h denote, respectively, the conduction band, the light hole band and the heavy hole band, $\uparrow,\downarrow$ indicate on spin states, N_s is the paramagnetic ion concentration, $\alpha = S\langle J|S\rangle$, $\beta = S\langle J|S\rangle$; $u_1, u_2, \ldots, u_6$ Bloch multipliers, $|S\rangle, |X\rangle$ are the atomic s and p functions.

From (5) to (15) we see that the exchange interaction leads to the splitting of the bands into spin bands. Using the obtained spectrum and wave functions, we calculated the differential cross section (DCS) of Raman scattering. Since, in the general case, it has a cumbersome form, we present below the expression of the DCS only for ZZ geometry.

3 Scattering spectrum

Fig.1a shows the zone structure of $Hg_{1-x}Mn_xTe$ SMS at point Γ (at small values of the concentration of magnetic ions Mn^{+2}, x=0.02) and a schematically possible process of interband electron Raman scattering (IERS). In the presence of a magnetic field, energy levels are split into spin sublevels due to exchange interaction. As a consequence, the number of possible processes increases to four; $(h\uparrow) \longrightarrow (c\uparrow), (h\downarrow) \longrightarrow (c\downarrow), (h\uparrow) \longrightarrow (c\downarrow), (h\downarrow) \longrightarrow (c\uparrow)$. These processes are shown schematically in Fig. 1b. For ZZ geometry, the IERS DCS has the following form:

$$\frac{d^2S}{d\Omega d\omega} = \frac{\sqrt{2}r_0^2 m_0^2 P^4 \mu^{3/2}}{45\pi^2\hbar^6} \cdot \frac{\omega_0 - \omega_1}{\omega_0} \left[K_1 + K_2 + K_3 + K_4\right], \tag{16}$$

$$K_1 = \left(\hbar\omega + \frac{2}{3}B\right)^{1/2} \cdot \left| \frac{1}{\varepsilon_g + \hbar\omega_0 - A + \frac{5}{3}B + \hbar\omega} + \frac{1}{\varepsilon_g - \hbar\omega_0 - A + \frac{5}{3}B + 2\hbar\omega} \right|^2, \tag{17}$$

$$K_2 = \left(\hbar\omega + \frac{4}{3}B\right)^{1/2} \cdot \left| \frac{1}{\varepsilon_g + \hbar\omega_0 - A + \frac{7}{3}B + \hbar\omega} + \frac{1}{\varepsilon_g - \hbar\omega_0 - A + \frac{7}{3}B + 2\hbar\omega} \right|^2, \tag{18}$$

$$K_3 = \left(\hbar\omega - \frac{4}{3}B\right)^{1/2} \cdot \left| \frac{1}{\varepsilon_g + \hbar\omega_0 - A + \frac{7}{3}B + \hbar\omega} + \frac{1}{\varepsilon_g - \hbar\omega_0 - A + \frac{7}{3}B + 2\hbar\omega} \right|^2, \tag{19}$$

$$K_4 = \left(\hbar\omega - \frac{2}{3}B\right)^{1/2} \cdot \left| \frac{1}{\varepsilon_g + \hbar\omega_0 - A + \frac{5}{3}B + \hbar\omega} + \frac{1}{\varepsilon_g - \hbar\omega_0 - A + \frac{5}{3}B + 2\hbar\omega} \right|^2. \tag{20}$$

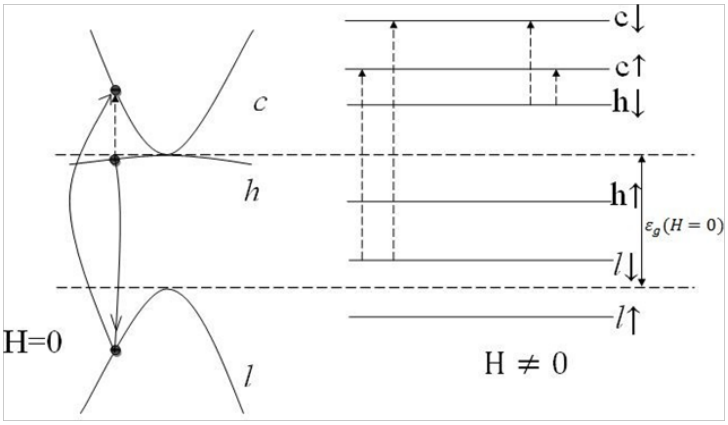

Figure 1: (a) Band structure of $Hg_{1-x}Mn_xTe$ at point G in the case H=0 and possible IERS process; (b) possible IERS processes in $Hg_{1-x}Mn_xTe$ in the case of H≠0.

In the usual case (Fluegel et al., 2015; Burstein et al., 1971) i.e., in a nonmagnetic semiconductor (when $A = 0$, $B = 0$), there is only one IERS process (h) → (c), whereas in the SMS

case there are four such processes (for $Hg_{1-x}Mn_xTe$ - $B < 0$): (h ↑) → (c ↑), (h ↓) → (c ↓), (h ↑) → (c ↓), (h ↓) → (c ↑).

At $\hbar\omega = \frac{4}{3}B$ there are two processes (h ↓) → (c ↑), (h ↓) → (c ↓) and with increasing magnetic field, at $\hbar\omega = \frac{4}{3}B$, processes (h ↑) → (c ↑), (h ↑) → (c ↓) are included. It follows from (17-20), that resonances take place at the frequencies

$$\hbar\omega_{R1} = \left(\hbar\omega_0 - \varepsilon_g + A - \frac{5}{3}B\right)/2, \tag{21}$$

$$\hbar\omega_{R2} = \left(\hbar\omega_0 - \varepsilon_g + A - \frac{7}{3}B\right)/2, \tag{22}$$

$$\hbar\omega_{R3} = \left(\hbar\omega_0 - \varepsilon_g + A + \frac{7}{3}B\right)/2, \tag{23}$$

$$\hbar\omega_{R4} = \left(\hbar\omega_0 - \varepsilon_g + A + \frac{5}{3}B\right)/2. \tag{24}$$

The resonance conditions contain the parameters ε_g, A and B. Hence it is possible to determine these parameters from the resonance frequency measured in the experiment.

4 Discussion of the results

Note that scattering can be either resonant ($\hbar\omega_0 > \varepsilon_g$) or non-resonant ($\hbar\omega_0 < \varepsilon_g$). (see formulas (16)). Let $\hbar\omega_0 < \varepsilon_g$. Fig. 2 shows the dependence of the DCS of IERS on the shear energy for this case. When plotting the graph, the following parameters were used following parameters:

$T = 4.2$ K, $H = 10^3$ Oe, $\hbar\omega_0 = 0.117$ eV, $x = 0.02$, $\varepsilon_g = 0.3$ eV, $N_s\alpha = 0.7$ eV, $N_s\beta = -1.4$ eV.

At $\hbar\omega_0 \leq (2/3)B$, two processes (h ↓) → (c ↑) (h ↓) → (c ↓) take place, and as the shift frequency increases, at $\hbar\omega_0 > (4/3)B$ the processes (h ↑) → (c ↑), (h ↑) → (c ↑), (h ↑) → (c ↓) are included and all the four processes participate in the scattering. With further growth of $\hbar\omega$ mines to zero, due to the factor $(\omega - \omega_0)/\omega_0$.

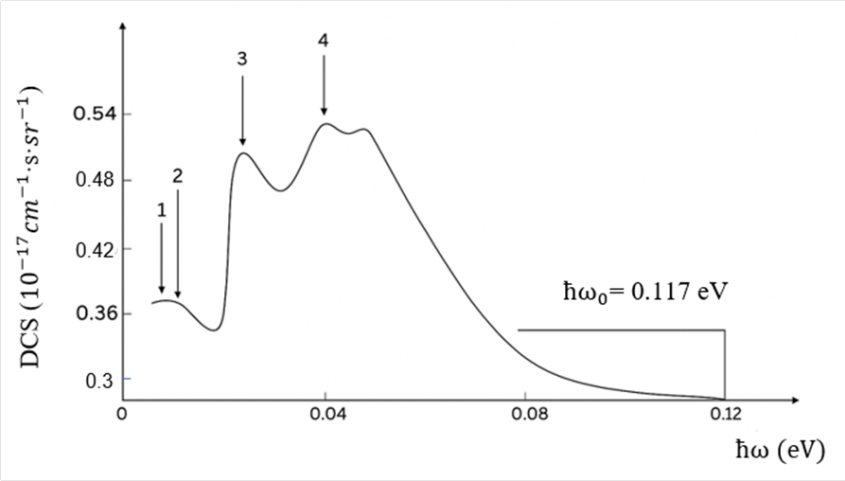

Figure 2: Dependence of IERS DCS on the shift energy for the non-resonant case in the $Hg_{0.98}Mn_{0.02}Te$ SMS at $H = 10^3$Oe. Scattering processes: 1. (h ↓) → (c ↑), 2. (h ↓) → (c ↓), 3. (h ↑) → (c ↑), 4. (h ↑) → (c ↓)

At $\hbar\omega_0 > \varepsilon_g$ scattering occurs resonantly and the resonance conditions are defined by formulas (16). It can be seen that, in contrast to a conventional semiconductor, which corresponds

to A=0, B=0, its one resonance peak is split into four resonance peaks. The frequencies of the resonances depend linearly on the concentration of magnetic ions. This allows us to determine the values of Nα and Nβ and, consequently, the ratio of the exchange parameters α and β from the values of the resonance frequencies.

With the help of formulas (16) it is possible to carry out comparative analysis of the magnetic ion concentrations, i.e., the positions of the resonance emission lines can be used to compare different samples and sort them by increasing ion concentrations. Even if ε_g and one of the parameters α or β are unknown, it is sufficient to record the resonance lines at two values of the magnetic field in order to determine the magnetic ion concentration.

A similar problem can be considered in the case of spin-flip Raman scattering (Walukiewicz, 1980; Rodina et al., 2020) as well as in the case of low-dimensional electron systems based on $Hg_{1-x}Mn_xTe$.

5 Conclusion

We have analyzed interband light scattering on electronic excitations in semimagnetic semiconductors $Hg_{1-x}Mn_xTe$ with inverted band structure under strong classical magnetic fields. The results allow comparison and classification of samples by magnetic ion concentration using the positions of the resonance lines. Even if one exchange parameter is unknown, the concentration can be extracted by measuring the spectra at two magnetic field values.

Raman scattering proves to be a highly effective tool for investigating the electronic and magnetic properties of semimagnetic semiconductors such as $Hg_{1-x}Mn_xTe$. One of its main advantages is that it is a non-destructive, contactless technique, allowing for the analysis of material properties without altering or damaging the sample. In this study, Raman spectroscopy enables the detection of fine spectral features, such as the splitting of interband resonance peaks, which directly reflect the strength of exchange interactions and the concentration of magnetic ions. This makes it possible to define key material parameters, including $N\alpha$ and $N\beta$, and to classify or compare samples based on their magnetic ion content. Additionally, the sensitivity of Raman scattering to external magnetic fields allows for further tuning and precise characterization, even when some parameters are unknown. These capabilities highlight Raman spectroscopy as a powerful method for materials diagnostics, quality control, and the development of spintronic and magneto-optical devices based on semimagnetic semiconductors.

References

Aleshkin, V.Ya., Domnina, O.L. & Zholudev, M.S. (2024). Electron-optical phonon scattering in the quantum well of a HgTe/CdHgTe heterostructure. *Physical Review B*, *109*, 075307.

Autieri, C., Śliwa, C., Islam, R., Cuono, G. & Dietl, T. (2020). Momentum-resolved spin splitting in Mn-doped trivial CdTe and topological HgTe semiconductors. *Physical Review B*, *103*, 115209.

Bastard, G., Rigaux, C. & Mucielski, A. (1977). Giant spin splitting induced by exchange interactions in $Hg_{1-k}Mn_kTe$ mixed crystals. *Physica Status Solidi (b)*, *79*, 585-593.

Betancourt-Riera, Re., Betancourt-Riera, Ri., Fernández-Lozada, M. & Ferrer-Moreno, L.A. (2025). Effect of electric field direction on electronic states and electron Raman scattering in ring-shaped semiconductor nanowires. *Physics Letters A*, *554*, 130707.

Betancourt-Riera, Re., Betancourt-Riera, Ri., Ferrer-Moreno, L.A., Fernández-Lozada, M. & Riera, R. (2023). Effects of an external electric field on one-phonon resonant and electron Raman scattering in a semiconductor quantum wire. *Materials Research Express*, *10*(11).

Burstein, E., Mills, D. & Wallis, R.F. (1971). Interband electronic Raman scattering in semimetals and semiconductors. *Physical Review B*, *4*, 2429-2437.

Cibert, J., Scalbert, D. (2017). Diluted Magnetic Semiconductors: Basic Physics and Optical Properties. In M. Dyakonov (Ed.). *Spin Physics in Semiconductors*, Springer Series in Solid-State Sciences, Vol. 157. Cham: Springer.

Dietl, T. (2021). From narrow-gap and semimagnetic semiconductors to spintronics and topological matter: A life with spins. *Acta Physica Polonica A*, *139*, 355.

Fernández-Lozada, M., Betancourt-Riera, Ri., Betancourt-Riera, Re., Ferrer-Moreno, L.A. & Riera-Aroche, R. (2021). Electric field to control light scattering on semiconductor QWW. *Optik*, *240*, 166849.

Fluegel, B., Mialitsin, A.V., Beaton, D.A., Reno, J.L., & Mascarenhas, A. (2015). Electronic Raman scattering as an ultra-sensitive probe of strain effects in semiconductors. *Nature Communications, 6*(1), 7136.

Furdyna, J.K., Dobrowolska, M. (2003). Coherent superposition of electric-and magnetic-dipole spin-flip transitions in zinc blende semiconductors. *Journal of superconductivity, 16*(4), 647-659.

Harrache, Y., Bouarissa, N. (2019). First-principles investigation of electronic structure and derived structural and magnetic properties of HgTe alloyed with Mn transition metal. *Solid State Communications*, *295*, 26-31.

Kyazym-Zade, A.G., Jafarov, M.A., Nasirov, E.F., Jahangirova, C.A., & Jafarli, R.S. (2017). Specific features of ZnCdS nanoparticles synthesized in different solvents. *Semiconductors, 51*(4), 454-457.

Miura, N. (2008). *Physics of Semiconductors in High Magnetic Fields*. New York: Oxford University Press.

Peng, Y., Li, X., Shi, L., Zhao, G., Zhang, J., Zhao, J., ... & Jin, C. (2025). A near room temperature curie temperature in a new type of diluted magnetic semiconductor $(Ba, K)(Zn, Mn)_2As_2$. *Advanced Physics Research, 4*(1), 2400124.

Rodina, A.V., Ivchenko, E.L. (2020). Theory of single and double electron spin flip Raman scattering in semiconductor nanoplatelets. *Physical Review B*, *102*, 235432.

Soares, T., Rodrigues, L., Moura, L., Ferreira, S., Mello, S., Sciammarella, P., Massardi, G. & Araujo, E. (2023). Effect of Mn concentration on the polar optical phonons frequencies in $Cd_{1-x}Mn_xTe$ thin films. *Applied Physics Letters*, *123*, 072103.

Teppe, F., Marcinkiewicz, M., Krishtopenko, S.S., Ruffenach, S., Consejo, C., Kadykov, A.M., ... & Dvoretskii, S.A. (2016). Temperature-driven massless Kane fermions in HgCdTe crystals. *Nature communications, 7*(1), 12576.

Walukiewicz, W. (1980). Spin-flip Raman scattering in semimagnetic semiconductors. *Physical Review B*, *22*(8), 3957.

Zawadzki, W. (1979). Narrow Gap Semiconductors Physics and Applications: Proceedings of the International Summer School Held in Nîmes, France, September 3-15. *Lecture Notes in Physics*, *133*.

Zeynalova, S.I., Ismayilov, T.H. (2024). Electron Raman scattering in $Hg_{1-x}Cd_xTe$ with inverted band structure. *Journal of Optoelectronics and Advanced Materials*, *26*(7-8), 335-340.